

## Chapter 2

# Neurovascular Geography and Mapping the Consequences of Its Injury

Ronald M. Lazar and Joanne R. Festa

As with any organ in the body, the brain depends upon the integrity of its blood supply to maintain normal function. Despite the fact that it only constitutes about 2% of body weight, however, it needs about 20% of the cardiac output and a comparable proportion of the total amount of oxygen used by the body. To understand the cognitive and behavioral consequences of an interruption of normal blood flow, it is important to provide first a general description of the geography of the cerebral circulatory system. The purpose of this chapter is to provide this overview and then to describe the diagnostic tools that reveal the effects of diseases and conditions that disrupt supply. For a more detailed anatomical description of this system and investigative modalities, the reader is referred to *Stroke: Pathophysiology, Diagnosis and Management* (Mohr, Choi, Grotta, Weir, & Wolf, 2004).

### Neurovascular Anatomy

The brain is fed by two main arterial sources: the internal carotid arteries and the vertebral arteries. The ascending aorta arises out of the

left ventricle of the heart and from the aortic arch come the brachiocephalic trunk and then the subclavian artery. From the brachiocephalic comes the carotid system with a left and right common carotid artery, and the subclavian artery, which gives rise to the left and right vertebral. Each common carotid artery splits, with the left and right internal carotid supplying the anterior cerebral circulation, about 80% of the brain's blood supply. The vertebral arteries unite at the border of the pons to form the basilar artery that supplies 20% of the brain's blood volume via the posterior cerebral circulation.

At the medial base of the cerebral hemispheres is a unique arterial ring, the circle of Willis, formed by early segments of the anterior, middle, and posterior cerebral arteries (PCAs) and the anterior and posterior communicating arteries. Figure 1 shows the distribution territories of the three major cerebral arteries.

The left and right anterior cerebral arteries (ACAs) arise from the anterior portion of the circle of Willis and are connected by the anterior communicating artery (ACoA). The ACoA, as well as small branches from the ACA, penetrate the brain to supply blood to the fornix, septal regions, anterior perforated substance, optic chiasm, optic tract, optic nerve, and suprachiasmatic area (Dunker & Harris, 1976). The ACA starts at the bifurcation of the internal carotid, entering the interhemispheric fissure, and then proceeding

---

R.M. Lazar (✉)

Stroke and Critical Care Division, Departments of Neurology and Neurological Surgery, Neurological Institute, New York Presbyterian Hospital, Columbia University, College of Physicians & Surgeons, New York, NY, USA

e-mail: ral22@columbia.edu

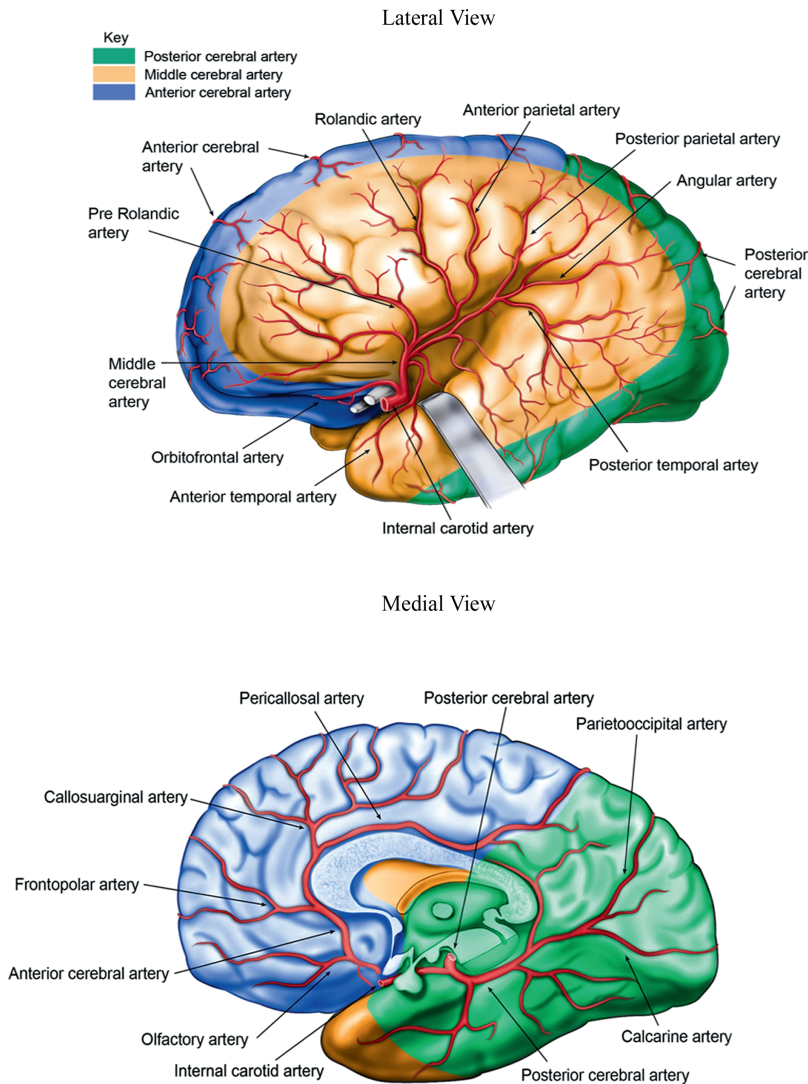


**Fig. 1** Lateral (above) and medial (below) views of the major arterial territories in the cerebral hemispheres. (From Festa, J. F., Lazar, R. M., Marshall, R. S., *Ischemic Stroke and Aphasic Disorders*, in *Ischemic*

*stroke and aphasic disorders*. In *Textbook of Clinical Neuropsychology*, J. E. Morgan, J. H. Rickers (eds). London: Taylor & Francis, 2008, with permission)

anteriorly and upward, and then posteriorly as it continues over the superior surface of the corpus callosum. Branches off the early segments of the ACA (e.g., Heubner's artery) supply the head of the caudate, the anterior part of the internal capsule, anterior globus pallidus, olfactory regions, and hypothalamus. The ACA gives rise to the medial striate artery, orbital branches, frontopolar branches, the pericallosal artery, and the callosomarginal

artery. Important brain regions supplied by these branches include the superior frontal gyrus, cingulate gyrus, and the premotor, motor, and sensory areas of the paracentral lobule.

The left and right middle cerebral arteries (MCAs) represent the largest of the major branches of the internal carotid arteries and supply most of the convex surface of the brain. Off the stem of the MCA are the

lenticulostriate branches, named for the structures comprising the lentiform nucleus and striatum (caudate and putamen), and the internal capsule. As the MCA begins its course over the cortical surface, it then subdivides into several different branch configurations, but the most common pattern is a bifurcation into an upper and lower division. The initial segments in these two divisions supply the insula region, before proceeding over a large expanse of the lateral surfaces of frontal, parietal, and temporal lobes, much in the fashion of a candelabra. In the upper, or superior, division there is supply to the frontal lobe, including the orbital region, the inferior and middle frontal gyri, the pre- and post-central gyri, as well as the superior and inferior parietal lobules. The lower or inferior division of the MCA provides circulation to the parietal and temporal opercula, the posterior temporal, posterior parietal, and temporo-occipital regions. The MCA can also exist in a trifurcation pattern so that the orbitofrontal, prefrontal, and precentral branches comprise an upper division, the rolandic, anterior parietal, and angular branches make up a middle division, and the inferior division mainly consists of supply to the temporal lobe, and to the temporo-occipital region (Mohr, Lazar, Marshall, & Hier, 2004).

The vertebral arteries, as they course up the spine into the skull, provide arterial supply to the brain stem and cerebellum, before merging into the basilar artery at the level of the pons. The posterior cerebral arteries (PCA's) are typically formed by the bifurcation of the basilar artery at the circle of Willis where they are connected by the posterior communicating artery (PCoA). The PCAs continue to course superiorly along the lateral part of the brainstem, with penetrators supplying segments of the thalamus, before turning posterior as they pass over the tentorium and onto the medial and inferior surfaces of the temporal and occipital lobes. The nomenclature for the cortical branches of the PCA seems to vary, but in general there are vessels that subdivide into those that feed the ventral temporal surface,

the occipito-temporal region, and those that supply the calcarine cortex. There is a variant of the PCA, called a "fetal" PCA, in which it arises directly from the internal carotid artery, and occurs in 5–10% of cases.

In addition to the three major cerebral arterial territory distributions, there are so-called "central arteries" that provide penetrating branches into deep brain. Among these are the anterior and posterior choroidal arteries. The anterior choroidal artery, usually arising from the internal carotid artery, courses from the lateral and then to the medial optic tract until the lateral geniculate body where it splits into many small branches before entering the temporal horn and the choroid plexus of the lateral ventricle. It supplies the optic tract, lateral geniculate body, medial temporal lobe, and the anterior one third of the hippocampus, the uncus, and part of the amygdala. Some of the perforating branches also feed the posterior limb of the internal capsule, optic radiations, the basal ganglia, and the ventrolateral region of the thalamus. Arising from the PCA, the posterior choroidal artery has one medial and two lateral branches and collectively feed superior and medial parts of the thalamus, the choroid plexus of the lateral ventricle, and the posterior two thirds of the hippocampus.

## Autoregulation

In order to survive, the neurons and supportive tissue in the brain rely on a steady supply of oxygen and glucose via the circulatory system. Autoregulation occurs so that neither too little (hypoperfusion) nor too much (hyperperfusion) supply occurs. Depending on the degree and duration of disruption of the cerebral blood supply, the neuron undergoes a well-described series of pathophysiological steps in metabolic function before permanent cell death, or infarction, takes place. To maintain adequate function as long as possible, there are compensatory mechanisms that take place in response to disrupted blood flow.

Under normal circumstances, about one third of the oxygen and one tenth of the glucose circulating through the brain's circulation is metabolized (Zazulia, Markham, & Power, 2004) so that there is a uniform fraction of the available oxygen and glucose utilized, based on the amount needed for the resting metabolic rate of tissue. Autoregulation is the brain's ability to maintain cerebral perfusion pressure (CPP) when oxygen and glucose are not sufficient to meet its metabolic needs. Protection against abnormal blood flow begins to occur when the partial pressure of oxygen in the blood falls to about 50–60 mmHg (Buck et al., 1998). When the CPP falls, CBF can be maintained by dilation of the cerebral arterioles and recruitment of collateral vascular channels (Marshall et al., 2001). Adequate blood flow across the circle of Willis, for example, can serve this purpose, either from the ACoA or the PCoA bringing flow from the vertebro-basilar system. The state of maximal vasodilation has been referred to as Stage I hemodynamic failure. If the CPP continues to fall and there is maximal dilatation of the arteries, autoregulation induces an increase in the oxygen extraction fraction (OEF). When the arterioles are maximally dilated and OEF is increasing, then Stage II hemodynamic failure, or "misery perfusion," is said to occur. If there is a restoration of normal CBF before OEF reaches its maximum level, then there can be good recovery of neuronal function. But once maximal OEF occurs, ischemia begins and has a direct impact on neuronal function. Even after 30 s of ischemia, glucose metabolism is reduced to 15% of normal levels (Pulsinelli, Levy, & Duffy, 1982). If ischemia occurs for a critical period of time, a breakdown of cell function will occur and neurons will sustain permanent injury or death. In human stroke, the CBF is very low in the ischemic core, but can be high enough in the surrounding region, known as the ischemic penumbra, so that hemodynamic rescue via thrombolysis (e.g., rTPA) or mechanical removal of clot may be achieved. In general, the brain can function for only 6–8 min if oxygen or glucose is reduced below critical levels.

## Diagnostic Studies

### *Brain Imaging*

Since there are multiple causes for similar clinical manifestations of neurological dysfunction, differentiating vascular from non-vascular causes (e.g., tumor, infection, demyelination), hemorrhage from ischemia, and ischemic subtypes is critical for diagnosis and treatment. Among diagnostic modalities, modern brain imaging represents a key investigative modality that can identify the presence of neurovascular diseases and conditions.

### Computerized Tomography

Computerized tomography (CT) of the brain is the most common imaging modality in cerebrovascular disease. Separating anatomy at different depths, a CT of the head uses moving sources of X-rays and detectors that measure the ability of tissue to block X-ray beams, with data that are reconstructed by computer into 5–7 mm slices oriented to the orbitomeatal plane, or about 15° from the horizontal plane. An example of a CT showing an ischemic stroke is shown in Fig. 2.

A CT scan of the head still represents the best way of distinguishing ischemic from hemorrhagic stroke: Low density signal attenuation suggests ischemia while high density indicates blood. Smaller hemorrhages may gradually lose signal intensity over 1 week but larger hemorrhages will produce high density signal changes that can persist for much longer durations. But within the acute period, the ability of CT to detect blood associated with parenchymal hemorrhage or subarachnoid hemorrhage makes it the radiographic modality of choice over MRI (Williams & Snow, 1995). The disadvantage of CT is that bone within the posterior fossa makes detection of signal changes in the brainstem more difficult.

With regard to ischemic brain injury, acute infarction can be detected as early as 3 h, with half of the cases positive at 12 h, and in some

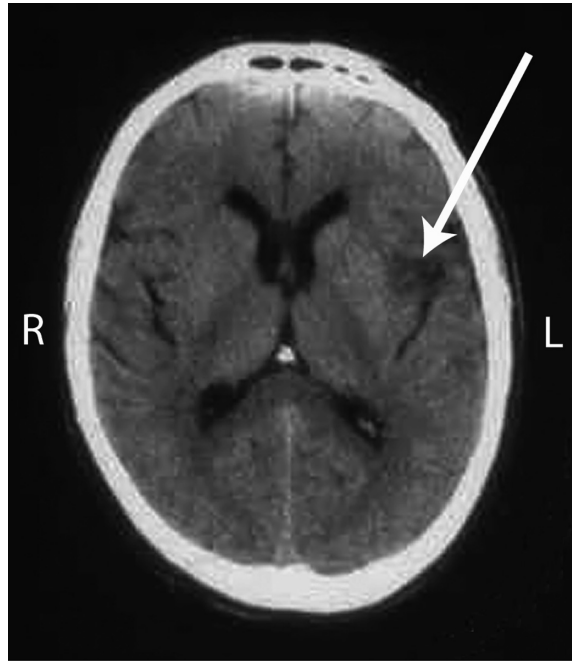


**Fig. 2** A computerized tomographic (CT) image of the head without injection of contrast material. The top of the figure represents anterior and the bottom posterior

locations in the brain. The arrow points to an ischemic infarct in the left hemisphere. L = Left, R = Right

instances, taking up to 3 days. But within 1 h after the onset of stroke symptoms, there is often loss of delineation between gray and white matter (Tomura et al., 1988). Ischemia resulting from embolic infarction seems more apparent on CT than ischemia associated with perfusion failure (Schuknecht, Ratzka, & Hofmann, 1990). With regard to the identification of ischemic changes in brain tissue supplied by small-vessel vessels, CT is capable of localizing injury as small as 1–2 mm.

### Magnetic Resonance Imaging

Magnetic resonance imaging (MRI) has become an important technique in the visualization of cerebrovascular disease because of its ability to depict the brain in any plane, including top to bottom (axial), side to side (sagittal), and front to back (coronal), and its superiority of resolution when compared to CT. Another advantage of MRI is that it does not use ionizing radiation or radioactive tracers.

The physics underlying MRI reveals that certain nuclei in tissue, mainly water and fat protons, when placed in a magnetic field align themselves with it. When radiofrequency (RF) pulses are then delivered, these nuclei absorb energy and then transfer energy back to a nearby detector coil at the same frequency. Over time, MR signal slowly fades away (relaxes) and the time constant for this decay varies in different tissues. The greater contrast resolution of MRI is based on its ability to detect the tissue-specific behavior of protons in different planes relative to the magnetic field. There are a number of different pulse sequences that have been used in MR imaging to assess cerebrovascular diseases and conditions; the most commonly used ones are described here. As of the moment, the magnetic strength of most clinical scanners ranges between 1.5 and 3.0 Tesla, although more powerful magnets, now used only for research, will likely be used in the future.

A  $T_1$ -weighted image (see Fig. 3, Left) is based on the relaxation time when protons

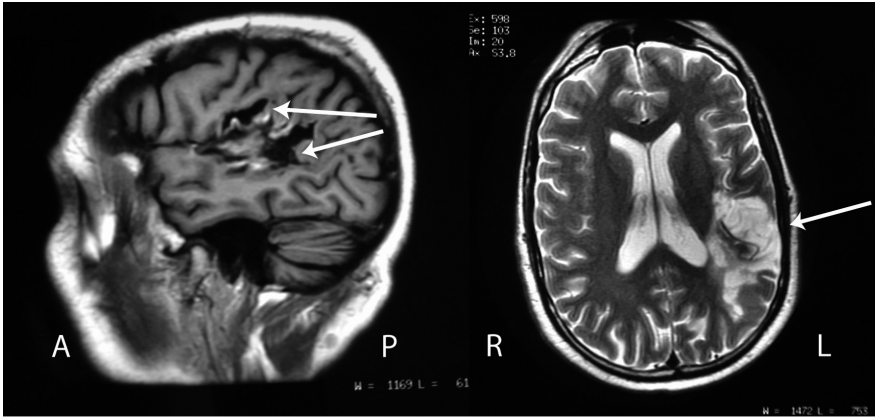


**Fig. 3** Magnetic resonance images (MRI) of the brain. The left panel is a sagittal (lateral view)  $T_1$ -weighted image of an ischemic infarct in the left hemisphere. A =

Anterior, P = Posterior. The right panel is an axial  $T_2$ -weighted image of the same infarct

are aligned with the main (longitudinal) magnetic field. The  $T_1$  image depicts white matter as brighter than gray matter. The cerebrospinal fluid (CSF) has low signal intensity so that it appears dark. Because of the water content in ischemic infarcts, it is therefore not surprising that they appear as hypointense on the  $T_1$  image. In general, anatomy is more clearly defined with this pulse sequence.

A  $T_2$ -weighted image (see Fig. 3, Right) is derived when the RF pulses are delivered to hydrogen protons whose rotational spins are

then flipped into the transverse plane relative to the main magnetic field.  $T_2$  relaxation refers to the energy emitted back from the protons as they become re-aligned with the main magnetic field. The  $T_2$  image shows CSF as a hyperintense (bright) signal. Ischemic brain lesions also appear hyperintense.

Fluid-attenuated inversion recovery (FLAIR) images (see Fig. 4, Left) involve the delivery of another RF pulse sequence that has the ability to suppress the CSF hyperintense signal so that it appears dark like in a  $T_1$

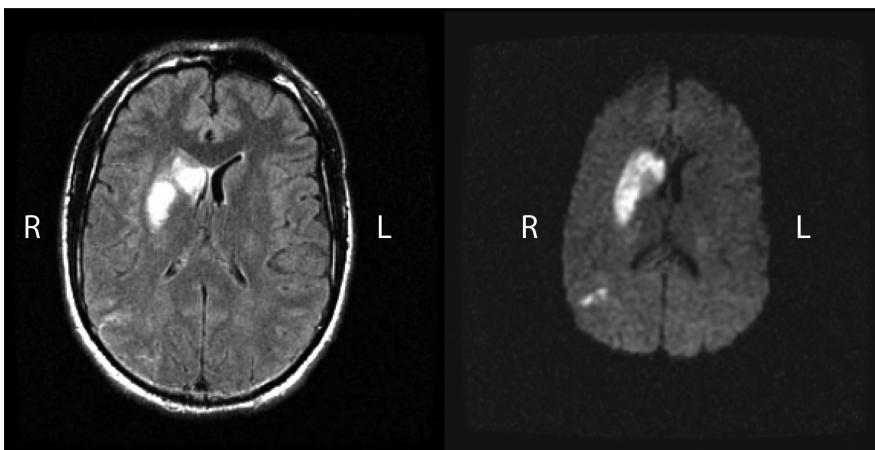


**Fig. 4** MRI of the brain. The left panel is an axial fluid-attenuated inversion recovery (FLAIR) image of a subcortical stroke in the right hemisphere. The right

panel is an axial, diffusion-weighted image (DWI) of the same clinical event

sequence but at the same time lesions appear bright like those in  $T_2$  images. The result is an image that shows with greater contrast the presence of lesions. Another advantage of FLAIR imaging is excellent visualization of extra-axial blood, such as might be seen in subarachnoid hemorrhage or subdural hematoma (Noguchi et al., 1994).

The development of *diffusion-weighted imaging (DWI)*, and more recently *perfusion-weighted imaging (PWI)*, have improved identification of stroke in the acute phase, leading to a better understanding of acute pathophysiology and improving decision-making in acute stroke management (see Fig. 4, Right). The detection of the DWI signal is based on the presence of cytotoxic edema in the extracellular space arising from ischemic tissue. Areas of hyperintensity most often represent areas of infarction. Comparing sensitivity in detecting acute clinical stroke within 3 h after symptoms onset, Chalela et al. showed that DWI was superior to CT (Chalela et al., 2007). The sensitivity of DWI is such that nearly one-half of transient ischemic attack cases, defined by negative CT and a syndrome lasting less than 24 h, are DWI positive and therefore are reclassified as ischemic stroke (Kidwell et al., 1999).

Requiring the intravenous injection of the contrast agent gadolinium, PWI has the property of detecting the total brain volume of hemodynamically-compromised tissue, regardless of whether it is infarcted or compromised by ischemia but capable of recovery (Quast, Huang, Hillman, & Kent, 1993; Schlaug et al., 1999). The signs and symptoms of acute stroke have been shown to correspond with the total region of hemodynamically-compromised tissue, without distinguishing between the infarcted and the ischemic, still viable brain tissue. By assessing the volume of infarcted tissue as defined by the DWI image, and subtracting that from the PWI image, the DWI/PWI mismatch provides a visual representation of the tissue that is compromised but still capable of returning to normal function if blood flow could be restored. This border zone

between infarcted tissue and normally-appearing tissue is commonly referred to as the “ischemic penumbra,” and is the target for acute reperfusion therapy. When reperfusion of the ischemic territory has taken place, either naturally or from intervention, the lingering clinical deficits correspond only to the residual region of infarction (Lee, Kannan, & Hillis, 2006).

One of the most recent developments in MRI sequencing is *diffusion tensor imaging (DTI)*. Although a thorough discussion of DTI is beyond the scope of this chapter, it takes advantage of edema detected in DWI by assessing the movement of water molecules in a region in which there are constraints in the direction of movement, such as in an intact white-matter tract in which the cell membrane constrains movement in the direction of that tract. The process of reconstructing the vector of the diffusion of these molecules is the basis of DTI tractography and holds promise for delineating the integrity of white matter in ischemic disease (Sotak, 2002).

Finally, another technique that holds promise in neurovascular disease but as yet largely remains investigative is *magnetic resonance spectroscopy (MRS)*, which measures the regional concentration of metabolites associated with, in this case, brain function. For example, Proton MRS has demonstrated that following middle cerebral artery stroke, there was a relative decrease in *N*-acetyl aspartate (associated with axonal myelin sheaths) and an increase in lactate in the regions of  $T_2$  hyperintensity, compared to the contralesional side (Gillard, Barker, van Zijl, Bryan, & Oppenheimer, 1996). More recently MRS, used to assess the efficacy of hyperbaric oxygen treatment for neuroprotection in acute stroke, demonstrated improved aerobic metabolism and preserved neuronal integrity (Singhal et al., 2007).

*Functional magnetic resonance imaging (fMRI)*, correlating some form of behavior during MRI with changes in oxygenated hemoglobin, is increasingly used in cerebrovascular disease and will be discussed in the chapter on stroke recovery (Chapter 17).

## Other Imaging Studies of Blood Flow and Metabolism

Single photon emission computed tomography (SPECT) involves the measurement of cerebral blood flow (CBF) in tomographic reconstruction of brain images following the injection of a radionuclide, most frequently  $^{99m}\text{Tc}$ -HMPAO. Alteration in CBF is thought to arise as a result its coupling to local brain metabolism and energy use, the pattern of which has been used to distinguish between dementia arising from Alzheimer's disease and that of vascular origin. More commonly, however, SPECT has been used to document CBF changes distal to stenosis or occlusion, or to visualize the effects of vascular anomalies, such as the brain arteriovenous malformation shown in Fig. 5(B). In this fashion, it becomes possible to dissociate the effects of focal ischemia arising from embolism from syndromes associated with perfusion failure from a more proximal location.

*Positron emission tomography (PET)*, like SPECT, requires the injection of a radioactive tracer isotope. Whereas CBF is an indirect measurement of brain metabolism in SPECT, PET directly assesses neuronal integrity. Unfortunately, the agent most commonly used for this purpose is fluorodeoxyglucose (FDG), a glucose compound containing a

radionuclide whose half-life is only a few hours and therefore requires a nearby cyclotron. PET can detect alterations in regional neuronal metabolism as well as determine the cerebral metabolic rate of oxygen. At this point, largely because of its limited availability, its application has largely been as a research tool with limited use in actual clinical practice in neurovascular disease.

## Cerebral Angiography

In contrast to imaging brain tissue, the role of angiography is to visualize the inside of major vessels supplying to or returning blood from the brain as well as the cerebral vessels within the brain itself. The purpose is to ascertain whether there are any physical restrictions that could impede normal flow and to determine the presence of anomalies such as aneurysms and vascular malformations. The three principal methods are catheter-based digital subtraction angiography (DSA), magnetic resonance angiography (MRA), and CT angiography (CTA).

In DSA (see Fig. 6), a short catheter, or sheath, is placed into the common femoral artery, allowing the introduction of smaller catheters and guidewires that allow catheterization of the aortic arch and ultimately the

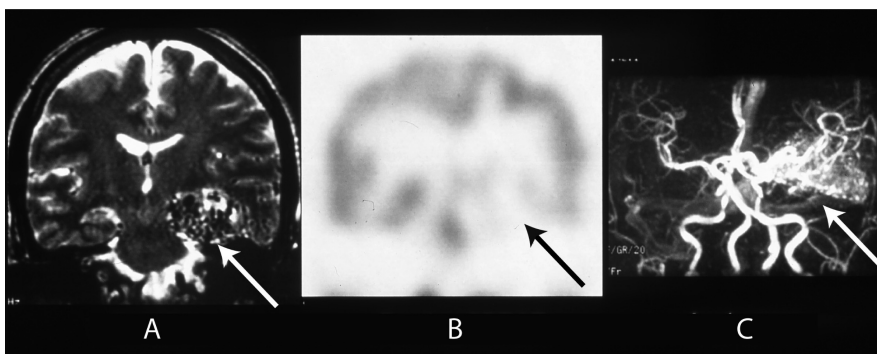


**Fig. 5** Three images depicting a left medial temporal arteriovenous malformation (AVM). (A) A coronal (front view)  $T_2$ -weighted image. (B) A single photon emission computed tomographic (SPECT) image

showing diminished cerebral blood flow in the left temporal region. (C) A magnetic resonance angiogram (MRA) of the brain AVM

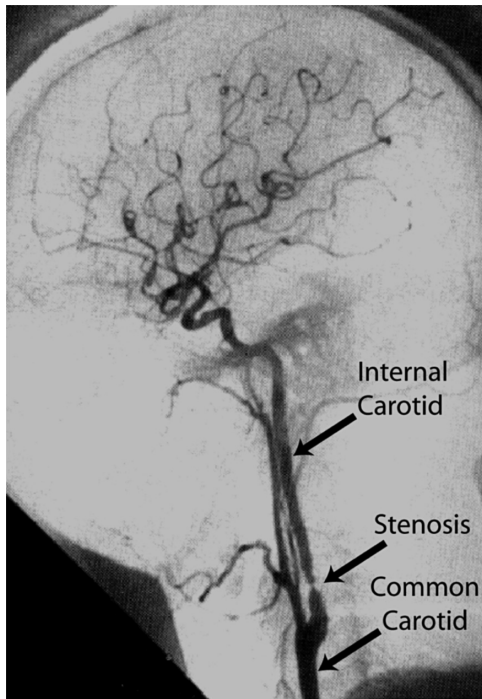


**Fig. 6** A cerebral angiogram of the left anterior circulation demonstrating a severe stenosis in the left internal carotid artery

carotid arteries and the anterior cerebral circulation, or the vertebrobasilar system and the posterior cerebral circulation. Contrast material which absorbs X-rays is injected at the target site, and the X-ray image maps the distribution of the contrast agent as it courses through the vascular territory. Superselective angiography entails the use of microcatheters, which can be placed further into the circulation and permit a more detail visualization of smaller defects. This technique represents the gold-standard of depicting vessels because of its high degree of resolution and its ability to show detail in vessels smaller than can be seen with any other angiographic method. There are, however, more risks associated with DSA. Among these include puncture of the blood-vessel wall, dislodgement of material adhered to the inner walls of vessels that can be carried downstream by the blood supply as emboli and cause ischemic stroke, and allergic reaction to the contrast agent. These risks have

been declining, mainly due to the development of new kinds of contrast materials and innovative catheter designs.

By changing the way RF pulses are delivered and the data are processed, it has become possible to use movement of blood to visualize large cerebral vessels during MRI, with the advantage that neither catheterization nor radiation is needed. MRA can render images in two dimensions, or as is more common, in three dimensions, which gives better spatial resolution (see Fig. 5c). In some settings, the comparability of conventional angiography and MRA is quite high.

Finally, new CT-based technology has enabled scanners to acquire blood flow data after the injection of a contrast agent. In addition to not requiring the use of a catheter, CTA has the significant advantage of being able to acquire images faster than other methods on scanners that are widely available.

### ***Duplex and Transcranial Doppler Ultrasonography***

First introduced in the 1970's, Doppler ultrasonography techniques are now commonly used to assess hemodynamics in the intracranial and extracranial arteries. A diagnostic imaging technology based on the analysis of high-frequency sound waves, Doppler ultrasonography is a rapid, non-invasive, portable, and low-cost means of assessing cerebral blood flow and is often employed as the initial screen for carotid disease and other suspected cerebrovascular disorders. Ultrasound can determine the patency of blood vessels, from stenosis to occlusion, the direction and velocities of blood flow through the vasculature, and the presence of vascular anomalies.

The Duplex test is a combination of ultrasound B-mode imaging, the black and white anatomic imaging, and color Doppler technology that can detect the movement of blood through the vessels by bouncing sound waves off blood cells. Using specified frequencies, the

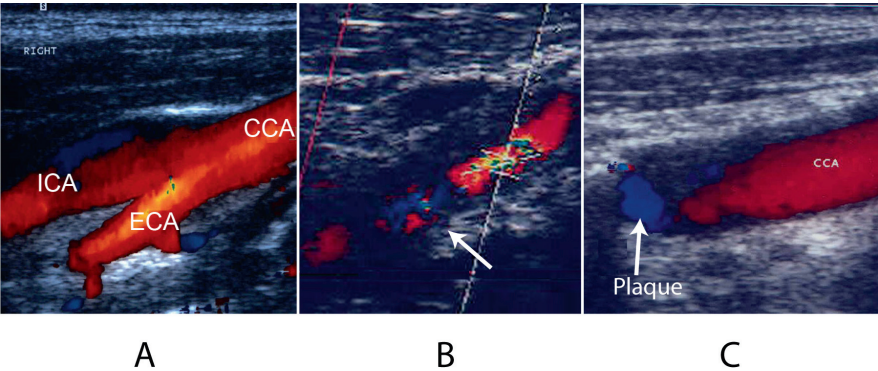


**Fig. 7** Duplex Doppler ultrasonography of the carotid bifurcation in three different patients. (A) Normal blood flow through the common carotid artery (CCA), internal carotid artery (ICA), and external

carotid artery (ECA) arteries; (B) blood flow through a stenotic segment of artery with arrow pointing to the area of stenosis; (C) total artery occlusion with arrow pointing to the occluding plaque

speed of blood flow in relation to the probe causes phase shifts with increases or decreases in sound frequency. The change in frequency directly correlates with the speed of blood flow. Typically used to assess the carotid and extra-cranial vertebral arteries, the Duplex test results in an image of the artery, any plaque causing stenosis, as well as a wave form that indicates blood velocity and other flow characteristics. Velocities determine the degree of artery stenosis and when no velocity is detected, the artery is considered occluded (see Fig. 7).

Transcranial Doppler (TCD) sonology uses the same technology to assess the intracranial vasculature through the transtemporal, trans-orbital, and transnuchal bone windows (see Fig. 8). The skull bones hamper ultrasound transmission so insonation of windows (areas

with thinner walls) must be utilized, such as the temporal region in front of the ear. Certain patient demographics, such as age, gender, and race affect bone thickness and composition, and thus the ability to obtain data. The ability to accurately locate target vessels through these windows is highly dependent on individual training and experience. TCDs can be useful in identifying intracranial stenosis or occlusion, evaluation of collateral circulation, detection of intracranial aneurysms and AVMs, detection of vasospasm in SAH, and assessment of cerebral autoregulation (Mohr, Choi et al., 2004). TCD monitoring may also be used in detecting microemboli entering the cerebral circulation from a proximal source such as the heart, or during vascular procedures.

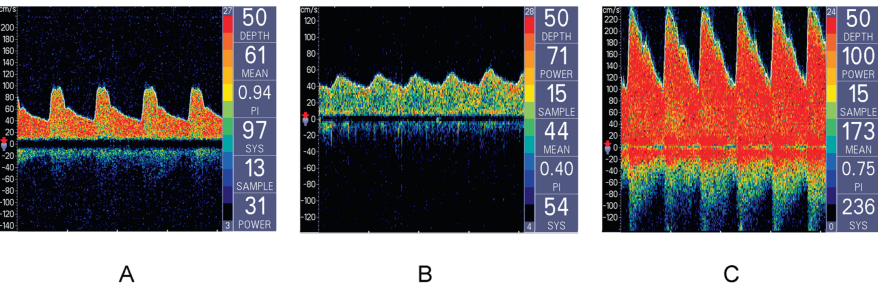


**Fig. 8** Transcranial Doppler (TCD) ultrasonography of the middle cerebral artery. (A) Normal wave form; (B) blunted wave form representing flow distal to a

stenosis; (C) accelerated wave form of flow through the stenotic segment of the vessel

## References

- Buck, A., Schirlo, C., Jasinsky, V., Weber, B., Burger, C., von Schulthess, G. K., et al. (1998). Changes of cerebral blood flow during short-term exposure to normobaric hypoxia. *Journal of Cerebral Blood Flow and Metabolism*, 18 (8), 906–910.
- Chalela, J. A., Kidwell, C. S., Nentwich, L. M., Luby, M., Butman, J. A., Demchuk, A. M., et al. (2007). Magnetic resonance imaging and computed tomography in emergency assessment of patients with suspected acute stroke: a prospective comparison. *Lancet*, 369 (9558), 293–298.
- Dunker, R. O., & Harris, A. B. (1976). Surgical anatomy of the proximal anterior cerebral artery. *Journal of Neurosurgery*, 44 (3), 359–367.
- Gillard, J. H., Barker, P. B., van Zijl, P. C., Bryan, R. N., & Oppenheimer, S. M. (1996). Proton MR spectroscopy in acute middle cerebral artery stroke. *AJNR American Journal of Neuroradiology*, 17 (5), 873–886.
- Kidwell, C. S., Alger, J. R., Di Salle, F., Starkman, S., Villablanca, P., Bentson, J., et al. (1999). Diffusion MRI in patients with transient ischemic attacks. *Stroke*, 30 (6), 1174–1180.
- Lee, A., Kannan, V., & Hillis, A. E. (2006). The contribution of neuroimaging to the study of language and aphasia. *Neuropsychology Review*, 16 (4), 171–183.
- Marshall, R. S., Lazar, R. M., Pile-Spellman, J., Young, W. L., Duong, D. H., Joshi, S., et al. (2001). Recovery of brain function during induced cerebral hypoperfusion. *Brain*, 124 (Pt 6), 1208–1217.
- Mohr, J. P., Choi, D. W., Grotta, J. C., Weir, B., & Wolf, P. A. (2004). *Stroke: Pathophysiology, diagnosis, and management* (4th ed.). New York: Churchill Livingstone.
- Mohr, J. P., Lazar, R. M., Marshall, R. S., & Hier, D. B. (2004). Middle cerebral artery disease. In J. P. Mohr, D. W. Choi, J. C. Grotta, B. Weir, & P. A. Wolf (Eds.), *Stroke: pathophysiology, diagnosis, and management* (4th ed.). New York: Churchill-Livingstone.
- Noguchi, K., Ogawa, T., Inugami, A., Toyoshima, H., Okudera, T., & Uemura, K. (1994). MR of acute subarachnoid hemorrhage: a preliminary report of fluid-attenuated inversion-recovery pulse sequences. *AJNR American Journal of Neuroradiology*, 15 (10), 1940–1943.
- Pulsinelli, W. A., Levy, D. E., & Duffy, T. E. (1982). Regional cerebral blood flow and glucose metabolism following transient forebrain ischemia. *Annals of Neurology*, 11 (5), 499–502.
- Quast, M. J., Huang, N. C., Hillman, G. R., & Kent, T. A. (1993). The evolution of acute stroke recorded by multimodal magnetic resonance imaging. *Magnetic Resonance Imaging*, 11 (4), 465–471.
- Schlaug, G., Benfield, A., Baird, A. E., Siewert, B., Lovblad, K. O., Parker, R. A., et al. (1999). The ischemic penumbra: operationally defined by diffusion and perfusion MRI. *Neurology*, 53 (7), 1528–1537.
- Schuknecht, B., Ratzka, M., & Hofmann, E. (1990). The “dense artery sign” – major cerebral artery thromboembolism demonstrated by computed tomography. *Neuroradiology*, 32 (2), 98–103.
- Singhal, A. B., Ratai, E., Benner, T., Vangel, M., Lee, V., Koroshetz, W. J., et al. (2007). Magnetic resonance spectroscopy study of oxygen therapy in ischemic stroke. *Stroke*, 38 (10), 2851–2854.
- Sotak, C. H. (2002). The role of diffusion tensor imaging in the evaluation of ischemic brain injury – a review. *NMR in Biomedicine*, 15 (7–8), 561–569.
- Tomura, N., Uemura, K., Inugami, A., Fujita, H., Higano, S., & Shishido, F. (1988). Early CT finding in cerebral infarction: obscuration of the lentiform nucleus. *Radiology*, 168 (2), 463–467.
- Williams, J. P., & Snow, R. D. (1995). Brain Imaging. In J. P. Mohr & J. C. Gautier (Eds.), *Guide to Clinical Neurology* (pp. 127–146.). New York: Churchill-Livingstone.
- Zazulia, A. R., Markham, J., & Power, W. J. (2004). Cerebral blood flow and metabolism in human cerebrovascular disease. In J. P. Mohr, D. W. Choi, J. C. Grotta, B. Weir, & P. A. Wolf (Eds.), *Stroke: Pathophysiology, Diagnosis, and Management* (4th ed., pp. 799–819). New York: Churchill-Livingstone.



Neurovascular Neuropsychology

Festa, J.; Lazar, R.M. (Eds.)

2009, XVI, 316 p. 46 illus., 5 illus. in color., Hardcover

ISBN: 978-0-387-70713-6